# Direct evidence of interchange between hole doping and Curie paramagnetism in underdoped $YBa_2Cu_3O_x$

J. Biscaras,[1] B. Leridon,[1] D. Colson,[2] A. Forget,[2] and P. Monod[1]

[1]*Laboratoire de Physique et d'Etude des Matériaux, UMR8213- CNRS-ESPCI ParisTech-UPMC, 10 rue Vauquelin, 75231 Paris Cedex 05, France*

[2]*Service de Physique de l'Etat Condensé, Orme des Merisiers, IRAMIS, CEA-Saclay (CNRS URA 2464), 91191 Gif sur Yvette Cedex, France*

(Received 18 November 2011; revised manuscript received 14 February 2012; published 16 April 2012)

We present high-accuracy magnetization measurements on $YBa_2Cu_3O_x$ ceramic samples, with $x$ ranging from 6.19 to 7.00. Magnetization relaxation measurements around or above room temperature display a cooling-rate-dependent behavior, evocative of a thermally activated mechanism. Through careful simultaneous time-dependent studies of the pseudogap and Curie law contributions to the magnetic susceptibility and of the critical temperature, we are able to establish an original, quantitative relationship between the proportion of free paramagnetic $Cu^{++}$, which is a measure of intrinsic oxygen disorder in the chains and the hole doping of the $CuO_2$ planes. This observation paves the way to a microscopic model for the role of charge "reservoir" played by the chains in $YBa_2Cu_3O_x$.

DOI: 10.1103/PhysRevB.85.134517 PACS number(s): 74.62.En, 74.62.−c, 74.62.Dh, 74.25.Ha

## I. INTRODUCTION

As the first high-temperature superconductor with its transition above nitrogen boiling point, $YBa_2Cu_3O_x$, with $x$ varying from 6.0 to 7.0, has been widely studied for its superconducting and pseudogap properties, but also for its somehow related particular structural behavior. Indeed, property changes common to all cuprate families (from antiferromagnetic Mott insulator to high-temperature superconductor) are accompanied in $YBa_2Cu_3O_x$ by structural changes (from tetragonal $T$ to orthorhombic OI) due to its particular charge reservoir: the CuO chains. In the following, we will denote YBCO$x$ for $YBa_2Cu_3O_x$.

From $x = 6.0$ to 7.0, the chain structure changes drastically, from a situation where oxygen is completely absent from the chain planes that are left only with oxygen-depleted copper squares, to a situation corresponding to fully filled Cu-O-Cu chains. In the intermediate doping, different kinds of order are possible, from fully disordered oxygen vacancies to, for special contents, regular alternance of full and empty chains. Chain ordering has been measured for various oxygen content and shows temperature-dependent structural transition $T$-OI, but also superstructure transitions[1] near selected oxygen contents, as similar chains tend to repulse each other. An example is the famous OII phase near $x = 6.5$ where, when ordered, one chain over two is filled and the other empty.

From the physical properties point of view, the underdoped part of the phase diagram of $YBa_2Cu_3O_x$ is, as for the other families of cuprates, the object of intense experimental studies. As a matter of fact, this intermediate region is resisting the two kinds of descriptions that are commonly used for such systems. The localized electron description suitable for the half-filling picture is no longer valid due to the large number of carriers that are added, and the Fermi-liquid description, appropriate for the overdoped systems, is proven to be unapplicable. Besides, the fermiology of these systems shows a marked depression in the density of states, named pseudogap, the nature of which is still under debate. Historically, this effect was first measured (but not pointed out) through a decrease in the magnetic susceptibility below a temperature $T*$ (Refs. 2 and 18 therein) and then through the $^{89}Y$ Knight shift decrease in NMR measurements.[3] It was then evidenced through various techniques, among which specific-heat measurements,[4] scanning tunneling microscopy (STM) studies, optical conductivity measurements, and angle-resolved photoemission studies (ARPES) (for a review, see Ref. 5 and references therein.) This decrease in the susceptibility below $T*$, usually attributed in a qualitative way to the pseudogap, appears to get more pronounced as the doping level is decreased.

Along the first susceptibility measurements was also noted the ubiquitous presence (for the YBCO system) of a paramagnetic Curie law contribution of variable amplitude attributed to the "free $Cu^{++}$" in the CuO *chains*. This term gets also more pronounced when the doping is reduced. Although underdoped $YBa_2Cu_3O_x$ had been widely studied in the early days through magnetic susceptibility measurements,[6,7] recent work[8] has evidenced a singular feature in the temperature derivative of the magnetic susceptibility in the pseudogap regime of several underdoped YBCO polycrystalline samples. This feature seems to arise at a temperature $T_1$ close to the temperature $T_{mag}$ at which another magnetic feature, namely, a staggered magnetic order, is seen by polarized neutron diffractions.[9–11] It is also to be noted that polar Kerr effect measurements show a rotation of the polarization of light[12] attributed to time-reversal-symmetry breaking, below a temperature lower than $T_{mag}$.

This paper is presented as follows. After describing the elaboration and characterization of the $YBa_2Cu_3O_x$ polycrystalline samples, we will present high-accuracy susceptibility measurements showing a dependence of the magnetization on the cooling rate. In particular, we will separate the effects of the cooling rate on the Curie law susceptibility and on the so-called "pseudogap" susceptibility (inspecting and discarding the possible contributions of parasitic phases to this effect) and finally on the critical temperature. Then, we will describe magnetic relaxation measurements as a function of time, carried out on $YBa_2Cu_3O_x$ samples at various doping. The variations with oxygen ordering of the Curie term susceptibility, usually attributed to "free" $Cu^{++}$ in the chains,

 

and of the magnitude of the pseudogap susceptibility will be quantitatively compared and shown to be intrinsically related. In the Appendix, we will also inspect the possibility that the evidenced structural disorder effects may induce anomalies in the susceptibility measured above room temperature.

## II. ELABORATION AND CHARACTERIZATION OF THE POLYCRYSTALLINE SAMPLES

The samples from three different batches were prepared and characterized at SPEC-CEA (Saclay, France). The $YBa_2Cu_3O_7$ powder was prepared from the appropriate mixture of $Y_2O_3$ (Fluka purity 99.98%), $BaCO_3$ (Strem 99.999%), and CuO (Strem 99.999%). The $Y_2O_3$ and $BaCO_3$ precursors had been beforehand dried at 400 °C during 12 h before synthesis. The reaction was performed in a step of 40 h at 940 °C and three times 12 h at 950 °C separated by grindings of the powder sample in order to obtain a homogeneous phase. Several treatments at high temperature were necessary to ensure a complete decomposition of the carbonate $BaCO_3$. Then, the mixed powder was pressed at 0.5 t/cm$^2$ into pellets of about 750 mg (about typically $10^{-3}$ mol) with dimensions of 6 mm diameter and 6 mm height, and heated at 950 °C during 6 h to ensure the sintering of the samples. Finally, the pellets were annealed under pure oxygen at 350 °C during 24 h. After this step, powder x-ray diffraction (XRD) was performed to control the purity of the samples. XRD patterns were recorded on a D8 advance diffractometer of Bruker-axs using CuK$\alpha$ radiation, between 20° and 70° with a counting time of 20 s per step. All the samples were found consistent with a single phase with orthorhombic structure. No traces of secondary phases such as CuO, $BaCuO_2$, or $Y_2BaCuO_5$ were detected with this technique. Samples with controlled oxygen content were prepared by annealing pellets from the same batch under appropriate conditions of temperature and $O_2$ pressure and quenching them in a nitrogen atmosphere. A Netzsch (STA449C) thermobalance was used, coupled with gas distribution systems delivering $N_2$-$O_2$ mixtures.

## III. EXPERIMENTS

### A. Experimental setup

We have studied the time dependence of the magnetization of eight YBCO$x$ polycrystalline[13] samples of various oxygen content, namely, $x = \{6.19, 6.28, 6.32, 6.43, 6.56, 6.73, 6.79, 7.00\}$ using a Quantum Design MPMS-5T (Magnetic Properties Measurement System) magnetometer. The different samples with their critical temperature $T_C$ whenever superconducting (determined for simplicity by the value of $T$ for which the magnetic susceptibility $\chi = 0$ at 1 T) are listed in Table 1 of Ref. 8. Upon decreasing the oxygen concentration in the sample and therefore the carrier concentration, the $T_C$ of the superconducting samples was varied from 90.7 K down to 30.7 K for five different samples, and three samples were made nonsuperconducting by decreasing the oxygen doping below $x = 0.4$.

The samples were held in a polyethylene straw and measured using the same protocol as the one described in previous work.[8] In general, the reproducibility over 5 to 10 scans of the magnetization measurements over warming or cooling could reach $10^{-7}$ emu or equivalently $10^{-8}\mu_B$ per copper atom, when nine scans were averaged out per measurement. But, the accuracy can be downgraded of about one order of magnitude when only one scan per measurement is performed. In addition, due to the variable cooling procedures, some slowly varying relaxations of the magnetization were observed as a function of time and temperature. We will carefully describe and analyze these effects in this paper.

Temperature sweeps are made using a resistive heater and a cold helium flow controlled by the MPMS program. This program allows linear temperature sweeps with rates up to 10 K/min, however, the faster sweeps need 4 to 5 K at start to get to their nominal cruise value. The sweeps end by a temperature overshoot (or undershoot), the amplitude of which grows with sweeping rate (4 K for the fastest 10 K/min sweeps). Only sweeps faster than 1 K/min show significant thermalization effects due to the chamber thermal dynamics. The measured temperature is that of the chamber and may present a small difference with the average sample temperature. Therefore, a special check was performed on a $x = 7.00$ disk in order to measure the thermal diffusivity within the sample using the photothermal "mirage effect."[14] This yielded a time constant of less than 10 s for our samples, much shorter than the typical time scale of the measurements described below.

### B. Effect of the cooling rate on the susceptibility

Temperature sweeps from 100 to 400 K under magnetic field of 1 T as described in Ref. 8 show the usual behavior of the magnetic susceptibility of $YBa_2Cu_3O_x$: a low-temperature paramagnetic Curie-type term attributable to paramagnetic $Cu^{++}$, and at high-temperature a term increasing with temperature, usually associated with the effect of the pseudogap state on a Pauli-type susceptibility (see Fig. 1).

The $T$-increasing term in the susceptibility has been first observed by Johnston in $La_{2-x}Sr_xCuO_{4-y}$ (Ref. 15) and very shortly after by Alloul and co-workers[3] with NMR in $YBa_2Cu_3O_x$. This was the origin of the discovery of the pseudogap. The fact that the susceptibility is not constant

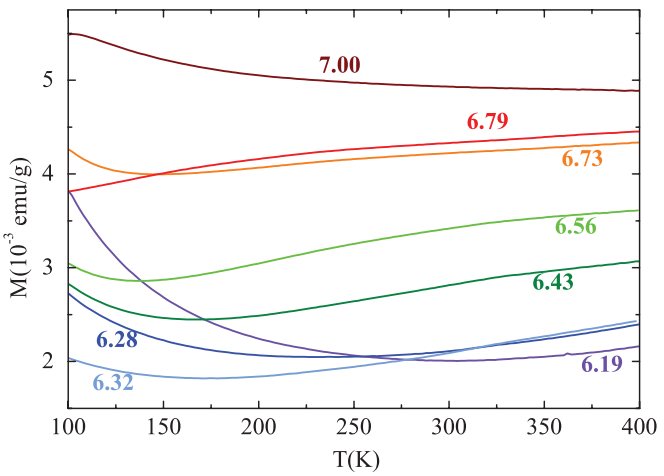


FIG. 1. (Color online) Magnetization between 100 and 400 K measured under 1 T in temperature sweeps of 1 K/min for the different samples. $x$ is indicated on each graph.

as a function of temperature as expected for a Pauli-type susceptibility in a Fermi liquid, but is found to drop below a certain temperature $T*$ is attributed to a loss in the density of states at the Fermi energy and therefore to the opening of the pseudogap.

This $T$-increasing term is observed in all the compounds *excepted in the optimally doped*. However, one should be aware that although this increasing term is also found for the extremely underdoped nonsuperconducting compounds, no other direct indication exists in that part of the phase diagram of the presence of a pseudogap. Actually, these strongly underdoped compounds are charge transfer insulators and antiferromagnets. The origin of the increasing suceptibility term may well be of a different nature in this case. An indication for this change of nature could be reflected by the apparent discontinuity observed in the room-temperature susceptibility of these compounds around $x = 6.4$ as was reported earlier.[8]

At lower temperature, a $T$-decreasing Curie law susceptibility attributed to the free $Cu^{++}$ present in the CuO chains is observed, getting more pronounced with lower oxygen content. It is to be noted that this term was previously observed in $YBa_2Cu_3O_x$.[2] However, the amplitude of the Curie-type term observed above 400 K in $La_{2-x}Sr_xCuO_{4-y}$,[15] where no chains are present, corresponds to *the total amount of Cu atoms in the material*, whereas the Curie term observed in our experiments (and subtracted out in Ref. 2) corresponds to about only 1% of the Cu atoms.

The susceptibility at low and intermediate temperature ($\leqslant$300 K) was found to depend on the temperature sweep rate (and not, within our accuracy, on the presence or absence of field during cooling). Therefore, in order to prevent artifacts caused by differences in sample thermalization at different cooling speed, samples were first warmed up to 400 K then cooled down under field to 100 K at the chosen cooling rate (1 K/min or 10 K/min) then stabilized at 100 K (1 h for maximum cooling speed, thermal effects are about 30 min long), before being measured from 100 to 400 K with 2-K temperature steps with averaging over nine scans per temperature (with an average warming rate of 0.5 K/min). The results for, respectively, fast and slow cooling rates were compared and are presented for sample YBCO*6.32* on Fig. 2.

Qualitatively, measurements over the eight oxygen contents show that for underdoped samples, after a fast cooling down, the amplitude of the low-temperature $T$-decreasing Curie term is larger and the amplitude of the $T$-increasing "pseudogap" term is smaller than after a slow cooling down. The difference between the two curves vanishes (within our accuracy) above a temperature close to 330 K. The relative difference $(M_{\text{fast}} - M_{\text{slow}})/(M_{\text{fast}} + M_{\text{slow}}) = \Delta M/M$ between the curves corresponding to fast and slow cooling rates was taken for the eight different samples and represented on Fig. 3. For all samples, excepted the optimally doped where no effect is noticeable, this difference is found to be positive at low temperature and then to become negative at a temperature generally decreasing with increasing doping level. Then, this difference increases again and finally goes to zero from negative values at a temperature around 330–340 K.

At 100 K, the amplitude of that difference is maximum for $x = 6.32$ and nonmeasurable at $x = 7.00$, and seems to follow

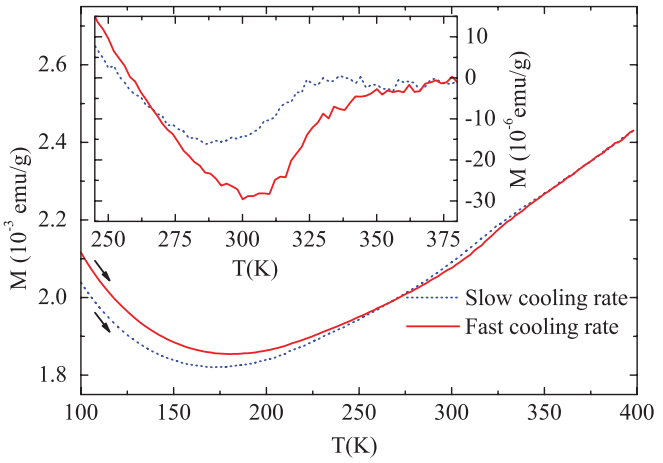


FIG. 2. (Color online) Magnetization measurements upon slow warming up (0.5 K/min) of sample YBCO*6.32* after, respectively, slow (1 K/min) cooling down (blue dotted line) and fast (10 K/min) cooling down (red solid line) from 400 K. Similar data are observed for all samples with $x < 7.0$. Note the crossing of the two curves circa 270 K. Inset: Same enlarged data between 250 and 380 K. Note that a linear trend has been subtracted from both curves in the inset.

a global trend with oxygen content (see Fig. 4). Therefore, although the effect is very weak (a few percent), it is unlikely to be caused by the different parasitic phases, nor by spurious handling.[16] The behavior of the relative difference $\Delta M/M$ for sample YBCO*6.32* in Fig. 3 is remarkable from several aspects. First, there is a marked angular point at around 312 K, which corresponds to the minimum of the curve. (Remarkably enough, it is very close to the Néel temperature expected for this compound[17] or to the OI-OII transition).[1] In addition, the relative difference decreases linearly from 100 to 312 K, whereas for concentrations lower than 6.32, the relative difference has a downward curvature and for higher concentrations it has an upward curvature. It is noteworthy that only sample 6.19 shows a constant value for $\Delta M/M$ at low temperature,

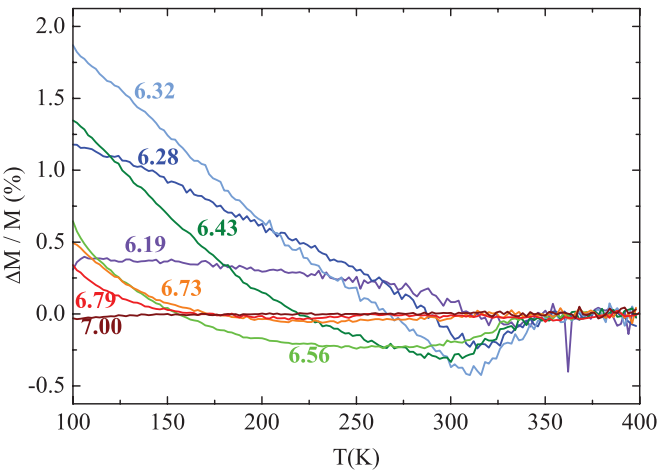


FIG. 3. (Color online) Relative difference $(M_{\text{fast}} - M_{\text{slow}})/(M_{\text{fast}} + M_{\text{slow}}) = \Delta M/M$ between the magnetic susceptibility of YBCO$x$ samples measured during slow warming up after temperature cooling down from 400 K with two different cooling rates: 10 K/min (fast) and 1 K/min (slow).

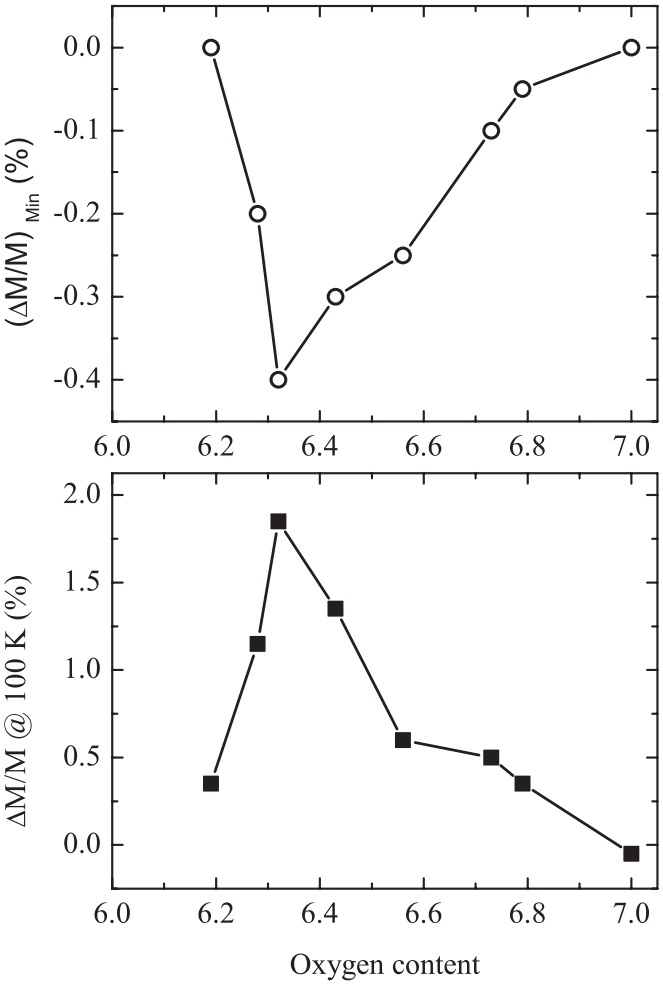


FIG. 4. Top: Amplitude of the relative difference $(M_{\text{fast}} - M_{\text{slow}})/(M_{\text{fast}} + M_{\text{slow}}) = \Delta M/M$ at its minimal (negative) value, giving the amplitude of the cooling rate effect in the "pseudogap" region, as a function of oxygen content $x$. Bottom: Amplitude of the relative difference $\Delta M/M$ at 100 K, giving the amplitude of the effect on the paramagnetic Curie term, as a function of the oxygen content $x$.

which is what is expected for the relative difference of two pure Curie contributions of different amplitudes.

Figure 4 shows the amplitude of the relative difference $\Delta M/M$ at 100 K as a function of the oxygen concentration $x$ (bottom), and the amplitude of $-\Delta M/M$ at its maximal value, corresponding to the maximal amplitude for the "pseudogap" contribution to $\chi$ as a function of $x$ (top). Both curves follow the same trend and, in both cases, go through a maximum of $|\Delta M/M|$ for $x = 6.32$, suggesting that the effect of a fast cooling down does simultaneously increase the Curie-type term and decrease the susceptibility in the "pseudogap" region.

### C. Contribution of parasitic phases to the susceptibility

As was reported in previous work[8] on the same samples, possible parasitic phases have been carefully investigated. The amount of $BaCuO_2$ could be determined by fitting the paramagnetic contribution in the optimally doped sample with a Curie-Weiss law ($\theta = 40$ K), to be only a few part per thousands.[2,8] The Curie contribution of the $Y_2BaCuO_5$ "green phase" is much smaller and was undetectable in our polycrystalline samples. The amount of $Y_2BaCuO_5$ was consistently shown to be less than 0.1%/mole through calibrated electron paramagnetic resonance measurements in the polycrystalline samples. The same cooling-rate protocol has been applied to single crystals with 30% of green phase and does not show larger cooling-rate-dependent effects.

Whereas the small Curie term in the optimally doped compound YBCO*7.00* can be fully attributed to $BaCuO_2$, in the underdoped samples this term is much larger, oxygen-content dependent, and therefore mostly attributable to the intrinsic "free" copper ions. In addition to these paramagnetic contributions, field sweeps from $-1$ T to $+1$ T at 150 and 400 K had previously revealed a well-characterized high-temperature ferromagnetic component equivalent to few ppm of parasitic iron-oxide phase. Field scans at 150 K after cooling from 400 K under two different cooling rates (1 and 10 K/min) show that the parasitic ferromagnetic component does not depend on the cooling rate.

We should also mention that, under very low field, a hitherto undetected magnetic transition was observed at 338 K in some of our samples (as well as in some YBCO single crystals) and attributed to the presence of $BaCu_3O_4$.[18] This phase gives a negligible contribution to the susceptibility at 1 T. We infer that the ubiquitous anticorrelated variation with doping content of both the "Curie" and the "pseudogap" contributions rules out an extrinsic origin for the reported effects.

### D. Effect of the cooling rate on the critical temperature

The superconducting transition temperature $T_C$, for the samples that were found superconducting, also showed a dependency with the cooling rate of underdoped samples (see Fig. 5). $T_C$ was determined by measuring under 15 G the diamagnetic susceptibility while warming from below $T_C$ at 1 K/min. For example, the $T_C$ of sample YBCO*6.43* is 3 K

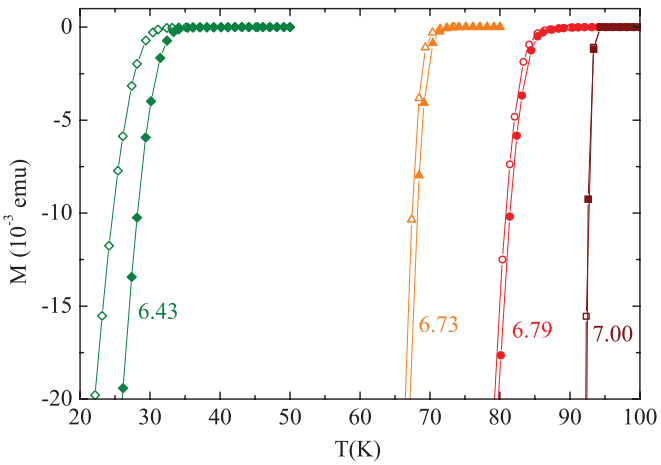


FIG. 5. (Color online) Superconducting diamagnetism under 15 G of four different YBCO$x$ samples after zero-field cooling down from 400 K with two different cooling rates. For every sample, the curve corresponding to the lower $T_C$ is obtained after the fast cooling down ($-10$ K/min, open symbols). Filled symbols: slow cooling rate ($-1$ K/min). No effect is measurable for $x = 7.00$.

lower when the sample is cooled at 10 K/min than at 1 K/min, whereas the $T_C$ of optimally doped YBCO*7.00* sample shows no measurable difference between the two thermal treatments. This effect had been previously observed by Refs. 19 and 20 and attributed to different ordering of oxygen vacancies in the chains above room temperature.

### E. Magnetization relaxation measurements

Since all these results suggest a relaxation process impacting simultaneously the critical temperature, the Curie-type term, and the "pesudogap" susceptibility, we have performed magnetic relaxation measurements under 1 T magnetic field as a function of time for four different samples among the eight, namely, YBCO*6.19*, YBCO*6.32*,YBCO*6.43*, and YBCO*6.56*. Samples were cooled down from 400 K at 10 K/min to a given relaxation temperature (chosen between 280 and 350 K), then the magnetization as a function of time was measured at this constant temperature. This magnetization is found to relax toward a slightly higher value.

Several protocols were tested to evaluate the effect of the sample chamber thermal dynamics on the measurements, and we finally retained the following: The sample was warmed to 400 K, then cooled down to the chosen temperature but at an off-centered position in the chamber (3 cm above the heater). This appeared to be a good compromise to avoid temperature gradients between the sample and the sample holder. Indeed, using this protocol, the magnetic relaxation appears qualitatively to proceed evenly in the first and in the following minutes. We do not report the first five minutes of the relaxation in the data presented here.

The relaxation of the magnetization as a function of time at different temperature is shown on Fig. 6 for sample YBCO*6.43*. It is to be noted that the noise here is significantly larger since only one scan was performed for every measurement, by contrast to the temperature sweeps presented above for which nine scans were averaged out for every temperature point. The noise level of the measurement allows different

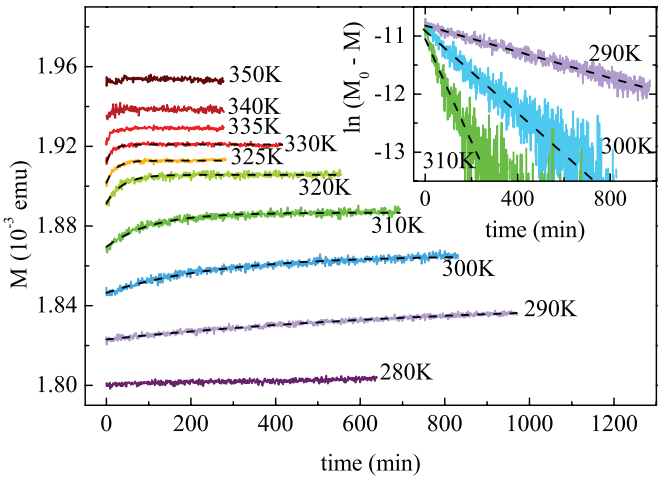


FIG. 6. (Color online) Magnetization relaxation measurements on YBCO*6.43* sample ($x = 6.43$) as a function of time. The dashed lines are the exponential fits to the data, for temperatures which allowed a reasonable fit. Inset, same data in log scale versus time for a chosen set of temperatures. $M_0$ denotes the magnetization at $t = \infty$.

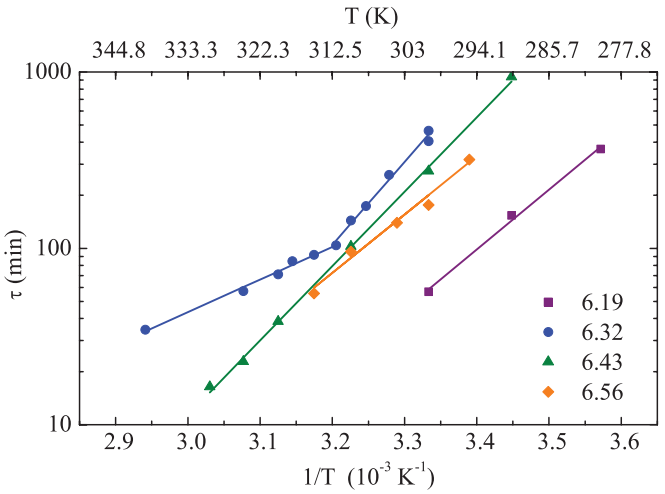


FIG. 7. (Color online) Relaxation times assuming an exponential relaxation for four different samples, as a function of the inverse of the temperature (markers) and corresponding Arrhénius fits using Eq. (1) of text (solid lines).

mathematical fits for the relaxations, however, the simplest model of an exponential relaxation (with a single relaxation time $\tau$) appears to be a satisfactory choice when all the experiments are being considered (see Fig. 6 and the inset.)

The behavior of the extracted relaxation time $\tau$ with respect to the temperature can be fitted to an Arrhenius law and seems to be thermally activated [see Eq. (1)]. The obtained relaxation times are plotted on Fig. 7. Activation energies are found to be about 0.5 to 1 eV for the different samples as may be seen on Fig. 8. The values of the relaxation times are consistent with previous observations:[20,21]

$$\tau = \tau_0 \exp\frac{\Delta}{k_B T}. \qquad (1)$$

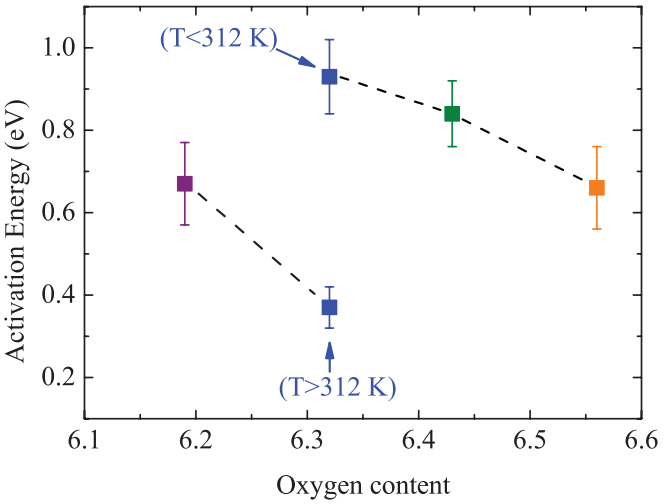


FIG. 8. (Color online) Activation energies ($\Delta$) deduced from a fit to an Arrhenius law [Eq. (1)] of the characteristic relaxation times $\tau$ (see Fig. 7). For sample YBCO*6.32*, two different activation energies are observed below and above 312 K. The dashed lines are a guide for the eye.

Note that for the oxygen content $x = 6.32$, two different activation energies are obtained below and above 312 K, which marks the position of either a structural or magnetic transition, as was noticed above. Low-temperature characteristics of the samples were measured during the course of a relaxation at 300 K by quenching the samples at 10 K/min, before warming them back up at 10 K/min to the relaxation temperature and repeating this process every hour. One-hour-long pieces of relaxation could then be pasted together and were shown to be identical to the relaxation measured without the quenches interruptions, which shows that the latter have no measurable effects on the relaxation behavior itself. The superconducting transition temperature and the amplitude of the Curie term were then measured during the different interruptions of a given relaxation for sample YBCO*6.43*.

### F. Discussion of the results from the quenching protocol

This quenching protocol actually allows (i) a quantitative estimate of the relation between the variation of the number of free $Cu^{++}$ in the chains $N$ and the variation of $T_C$, and (ii) a quantitative relation between the variations of $N$ and $p$, assuming a relation between $T_C$ and the doping level $p$.[22] Since a free $Cu^{++}$ is most probably present at the end of an interrupted chain, the number of free Cu is therefore a measure of the degree of disorder in the chains. For in an ideal $x = 7.0$ or 6.5 (stoichiometric OII) perfectly ordered phase, no free Cu should be present. See, for example, Ref. 1.

The Curie constant extracted from the low-temperature Curie term is related to the variation of the number of paramagnetic coppers per unit cell $N$ by

$$C = \frac{g^2 \mu_B{}^2 S(S+1)}{3k_B} N. \qquad (2)$$

We then relate the variations of $N$ to the variations of $T_C$, for $T_C \simeq 30$ K and $N \simeq 0.023$ both obtained from the quenching protocol, yielding a linearized relation for sample YBCO*6.43*: $\Delta T_C = \alpha_B \Delta N$, where $\alpha_B \simeq -23$ K/%$Cu^{++}$ $\pm$ 5 K.

Remarkably enough, this linearized relation extrapolated down to $N = 0$ (which corresponds to zero disorder in the chains of a sample of nominal oxygen content $x = 6.43$) gives $T_C$ of the order of 90–100 K. Actually, the Abrikosov-Gorkov mechanism *would precisely lead to a linear variation of* $T_C$ *with pair-breaking parameter* between $T_C^{\max}$ and $0.3T_C^{\max}$, suggesting that oxygen disorder in the chains may act as a pair-breaking parameter *à la* Abrikosov-Gorkov in the $CuO_2$ planes. If this assumption is true, it would also be an indication that the mechanism for oxygen doping in such compounds is essentially a variation of the amount of statistical disorder among the O atoms in the chains.

Using Liang's approximation of hole doping in $CuO_2$ planes,[22] we have then deduced the hole-doping variation from the $T_C$ variation measured through this quenching protocol. Figure 9 shows the relation between $N$ and the hole doping per unit cell $p$. The solid line corresponds to $4\Delta N = -\Delta p$, which is to be related to the fact that one CuO chain plane corresponds to two $CuO_2$ planes. This constitutes the first attempt to establish a quantitative relationship between the order in the chains, characterized by $N$ the number of paramagnetic $Cu^{++}$, closely related the number of chain ends, measured from the amplitude of the Curie term, and the hole doping in the planes $p$, characterized by $T_C$. It was already visible in Fig. 2 that when the amplitude of the Curie term increases (more free $Cu^{++}$), the "pseudogap susceptibility" amplitude decreases (less holes in the planes), but the graph in Fig. 9 allows us to give a quantitative estimate for this relationship.

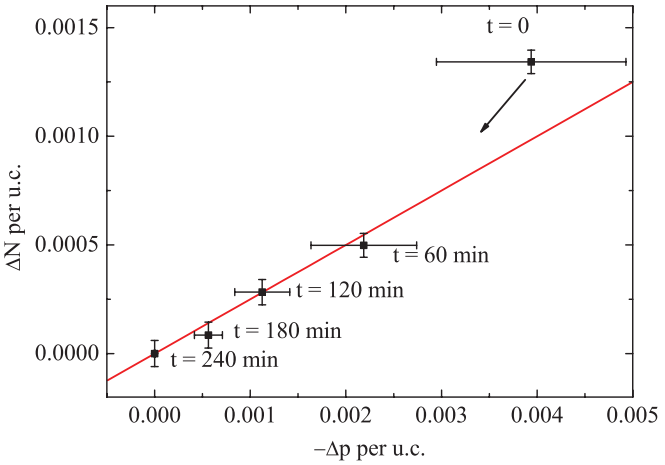


FIG. 9. (Color online) Relationship between the variation of the number of free Cu $N$ per unit cell and the hole doping $p$ during a given relaxation interrupted every hour in order to measure $T_C$ and the amplitude of the Curie term for sample YBCO*6.43*. The amplitude of the Curie term gives $\Delta N$, while $T_C$ yields the variation of the hole doping $\Delta p$ (see Ref. 22). The solid line corresponds to $4\Delta N = -\Delta p$. The arrow indicates the chronological order of the measurements.

An additional correlation can be established: When the variation of charge transfer observed after 4 h is $\Delta p = 0.004$ (deduced from the $T_C$ variation), the corresponding magnetization in the pseudogap state is found to vary by about 0.4% as well, which in a crude model would mean that the variation of the density of states at the Fermi energy $n(\epsilon_F)$ is also of 0.4%, so about the variation of $p$. This gives an indication of the variation of the density of states with $p$ within this range of doping.

## IV. CONCLUSIONS

Cooling-rate-dependent and time-dependent measurements of the magnetization of underdoped $YBa_2Cu_3O_x$ polycrystalline samples have evidenced relaxation effects above or around room temperature, leading to a change in the doping level of the $CuO_2$ planes. This is shown to have threefold consequences: (i) As is well known, on the value of $T_C$ whenever the sample is superconducting, and as is shown here (ii) on the amplitude of the Curie term at low temperatures, and (iii) on the amplitude of the "pseudogap susceptibility," i.e., the increasing part of the susceptibility usually ascribed to the existence of a pseudogap in the density of states.

An original, quantitative relationship has been established between the order in the chains, through the number of paramagnetic $Cu^{++}$ giving rise to Curie susceptibility and the number of holes in the $CuO_2$ planes, through $T_C$. Although these effects are expected to be ubiquitous in underdoped YBCO samples, this is, to our knowledge, the clearest appearance of a signature of the chain ordering in the magnetic susceptibility. Actually,

previous measurements of the resistivity and Hall effects up to 400 K show noticeable (but uncommented) singular points for the most underdoped samples that could be of the same origin (see Figs. 3 and 7 for the samples $\delta = 0.39$ and 0.53 in Ref. 23). This also leads us to reconsider with greater caution the determination of previously measured $T_1$ at which a discontinuity in the derivative of the susceptibility is observed (see Ref. 8) only for samples where it is found around or above room temperature, i.e., for oxygen content $x < 6.53$. See to this respect the Appendix of this paper.

These results illustrate, once more, the complexity and the specificity of, among all cuprates, the $YBa_2Cu_3O_x$ system where both $CuO_2$ planes and CuO chains of copper oxide are present, and are shown to interplay in a rather nontrivial way.

## ACKNOWLEDGMENTS

We gratefully acknowledge D. Fournier for photothermal measurements J. F. Marucco and C. Cochet for experimental contribution. This work was supported through a SESAME grant from Region Ile-de-France.

## APPENDIX: ORDER PARAMETER FREEZING

The fact that the typical relaxation times are in the range of 10–100 min above room temperature (see Fig. 7) is an indication that the order in the chains may affect the density of electrons in the planes and lead to different $p$ values according to the cooling procedure. Then, it is to be expected that the warming curves obtained for different cooling rates for a given sample should be identical at high temperature when the relaxation times are short enough for the order to be at its equilibrium value, and should split at low temperature, each of them corresponding to a different cooling-rate-dependent value of $p$. This is precisely observed in Fig. 2. In other words, temperature scans cover two qualitatively different behaviors: at low temperatures, the order parameter is frozen (and its value is higher when cooled down slowly); at high temperatures, the order parameter is at equilibrium and varies with temperature. These two domains correspond to situations where, respectively, the relaxation time is much larger or much shorter than the typical measuring and cooling times, and the separation temperature ($T_{th}$) between these two domains is around 300–320 K.

Since for strongly underdoped samples ($x < 6.53$) the temperature $T_1$ (Ref. 8) and $T_{th}$ are very close, we have examined the possibility that such a discontinuity may indeed be induced at $T_{th}$. For this, we have modeled the order in the chains with an order parameter $P$, $P_{TH}(T)$ being its thermodynamic value. In the simplest model (the relaxation time approximation), when $P$ is driven away from its thermodynamic value, it relaxes with a single relaxation time following Eq. (A1):

$$\frac{dP}{dt} = \frac{P_{TH}(T) - P(t)}{\tau(T)}. \tag{A1}$$

Numerical solution of this equation with an arbitrary $P_{TH}$ and measured relaxation times shows that our temperature scans induce a freezing of the order parameter while cooling, and a melting while warming. The freezing temperature is found to be around 320 K. Two $M(T)$ curves obtained by slow field

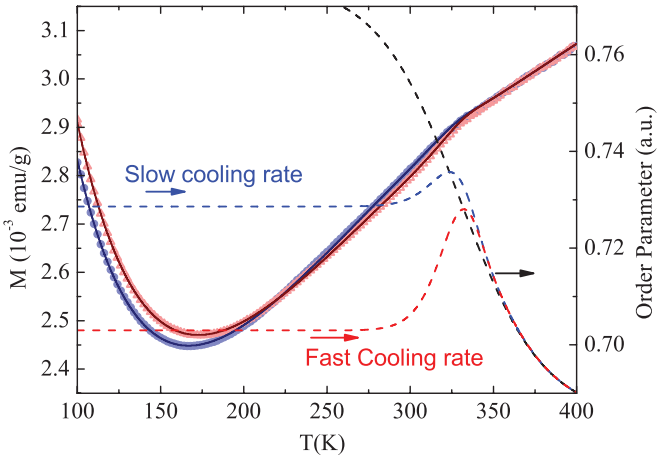


FIG. 10. (Color online) Left axis. Light red triangles and light blue circles: measured magnetization during warming of sample YBCO*6.43* after, respectively, fast and slow cooling rates. Dark red and dark blue solid lines: low-temperature fit and high-temperature extrapolation of the magnetization for, respectively, fast and slow cooling rate data. Right axis. Black dashed line: thermodynamical order parameter (explicitly chosen to reproduce the change of slope), red and blue dashed lines: realistic order parameters (blocked at low $T$, thermodynamical at high $T$), computed using the measured relaxation times, for, respectively, fast and slow cooling rates.

warming (0.5 K/min) after two different cooling treatments (1 and 10 K/min) for the same sample (YBCO*6.43*) were fitted using the empirical equation [Eq. (A2)] for the susceptibility[24] in the temperature range 100–300 K:

$$M(T) = A + \frac{B}{\cosh(T_0/T)} + \frac{C}{T}. \tag{A2}$$

Making the approximation that the magnetization varies linearly with respect to the order parameter, we can then extrapolate the computed magnetization at high temperatures. It appears that the melting of the order parameter may give a break in the slope of the magnetization above 300 K, as can be seen on Fig. 10. Since the order parameter is expected to be at thermodynamical equilibrium at high temperature, one is able to retrieve, from the experimental points, the thermodynamical order parameter. The results of the simulation are given on Fig. 10. The order parameter, which is necessary to simulate the high-temperature magnetization variation, is represented on Fig. 10 right axis. Consistently with early work on room-temperature annealing,[19,21] this order parameter could be related to chain ordering in underdoped samples. It is noteworthy that the extracted shape is strongly dependent on the variation that was assumed for the pseudogap susceptibility below 300 K and hypothesized to be still valid above 300 K [Eq. (A2)]. Moreover, this order parameter *is explicitly computed in order to produce the change in the slope*, therefore this does not constitute a proof that the observed change is due to oxygen diffusion effects, but only that such mechanism is possible in this range of temperature.

Besides, this simulation, done on only one sample, has to be taken carefully since the empirical equation (A2) does not have any theoretical background, and an assumption of linear dependence of the magnetization with the order

parameter has been made. However, this leads to reconsider with greater caution the interpretation of the anomalies present around or above 320 K in some of the underdoped samples ($x = 6.43$–$6.53$).[8] There is a possibility that for the oxygen contents lower than 6.53, $T_{th}$ was mistaken for $T_1$,[8] or that the two effects were indistinguishable, taking place at the same temperature. [The actual temperature $T_1$ could also be substantially lower for these strongly underdoped samples, as suggested on Fig. 5(b) of Ref. 8 for sample 6.43.]


[1] N. Andersen, M. von Zimmermann, T. Frello, M. Kall, D. Mønster, P.-A. Lindgard, J. Madsen, T. Niemoller, H. Poulsen, O. Schmidt *et al.*, Phys. C (Amsterdam) **317-318**, 259 (1999).

[2] J. Tranquada, A. Moudden, A. Goldman, P. Zolliker, D. Cox, G. Shirane, S. Sihha, D. Vaknin, D. Johnston, M. S. Alvarez *et al.*, Phys. Rev. B **38**, 2477 (1988).

[3] K. S. Hirata *et al.*, Phys. Rev. Lett. **63**, 16 (1989).

[4] W. Liang, J. Loram, K. Mirza, N. Athanassopoulou, and J. Cooper, Phys. C (Amsterdam) **263**, 277 (1996).

[5] T. Timusk and B. Statt, Rep. Prog. Phys. **62**, 61 (1999).

[6] M. Jurgens, Ph.D. thesis, Rijks Universiteit Leiden, 1990.

[7] D. Johnston, S. Sinha, A. Jacobson, and J. Newsam, Phys. C (Amsterdam) **153**, 572 (1988).

[8] B. Leridon, P. Monod, D. Colson, and A. Forget, Europhys. Lett. **87**, 17011 (2009).

[9] B. Fauque, Y. Sidis, V. Hinkov, S. Pailhes, C. T. Lin, X. Chaud, and P. Bourges, Phys. Rev. Lett. **96**, 197001 (2006).

[10] H. A. Mook, Y. Sidis, B. Fauqué, V. Balédent, and P. Bourges, Phys. Rev. B **78**, 020506 (2008).

[11] Y. Li, V. Baledent, N. Barisic, Y. Cho, B. Fauque, Y. Sidis, G. Yu, X. Zhao, P. Bourges, and M. Greven, Nature (London) **455**, 372 (2008).

[12] J. Xia, E. Schemm, G. Deutscher, S. A. Kivelson, D. A. Bonn, W. N. Hardy, R. Liang, W. Siemons, G. Koster, M. M. Fejer *et al.*, Phys. Rev. Lett. **100**, 127002 (2008).

[13] Typical size of the crystallites is about 30 $\mu$m.

[14] A. C. Boccara, D. Fournier, W. Jackson, and N. M. Amer, Opt. Lett. **5**, 377 (1980).

[15] D. Johnston, Phys. Rev. Lett. **62**, 957 (1989).

[16] M. A. Garcia, E. F. Pinel, J. de la Venta, A. Quesada, V. Bouzas, J. F. Fernández, J. J. Romero, and M. S. M. G. J. L. Costa-Krämer, J. Appl. Phys. **105**, 013925 (2009).

[17] J. Rossat-Mignod, L. Regnault, P. Bourges, P. Burlet, C. Vettier, and J. Henry, Phys. C (Amsterdam) **192**, 109 (1993).

[18] C. W. Rischau, B. Leridon, D. Colson, A. Forget, and P. Monod, Phys. Rev. B **85**, 134518 (2012).

[19] B. W. Veal, A. P. Paulikas, H. You, H. Shi, Y. Fang, and J. W. Downey, Phys. Rev. B **42**, 6305 (1990).

[20] H. Shaked, J. D. Jorgensen, B. A. Hunter, R. L. Hitterman, A. P. Paulikas, and B. W. Veal, Phys. Rev. B **51**, 547 (1995).

[21] P. Schleger, R. A. Hadfield, H. Casalta, N. H. Andersen, H. F. Poulsen, M. vonZimmermann, J. R. Schneider, R. Liang, P. Dosanjh, and W. N. Hardy, Phys. Rev. Lett. **74**, 1446 (1995).

[22] R. Liang, D. A. Bonn, and W. N. Hardy, Phys. Rev. B **73**, 180505(R) (2006).

[23] A. Carrington, D. J. C. Walker, A. P. Mackenzie, and J. R. Cooper, Phys. Rev. B **48**, 13051 (1993).

[24] Y. Lubashevsky and A. Keren, Phys. Rev. B **78**, 020505(R) (2008).